Journal of Applied Fluid Mechanics, Vol. 17, No. 11, pp. 2401-2410, 2024.
Available online at www.jafmonline.net, ISSN 1735-3572, EISSN 1735-3645.
https://doi.org/10.47176/jafm.17.11.2602

Stabilizing Pipe Flow by Flattening the Velocity Profile

C. Q. Zhou[1,2], H. L. Zhao[3] and H. S. Dou[1†]

[1] *Faculty of Mechanical Engineering, Zhejiang Sci-Tech University, Hangzhou, Zhejiang, 310018, China*
[2] *School of Mechanical and Automotive Engineering, Zhejiang University of Water Resources and Electric Power, Hangzhou, Zhejiang, 310018, China*
[3] *College of Aeronautics, Guizhou Vocational Technology Institute, Guiyang, Guizhou, 550023, China*

†*Corresponding Author Email: huashudou@zstu.edu.cn*

ABSTRACT

It is important to control turbulence in industrial processes. Past experimental and numerical researches have shown that a turbulent puff in pipe flow can be removed or delayed by flattening the profile of the upstream velocity because a flattened velocity profile causes the point of inflection on it to collapse. The energy gradient theory has been developed to study turbulent transition, and the relevant studies have shown that turbulence arises due to the generation of singularities in the flow field. In pressure-driven flows like the pipe flow, the point of inflection on the velocity profile leads to the appearance of a singular point in the unsteady Navier–Stokes equation. In this study, the energy gradient theory is used to demonstrate why the point of inflection on the profile of velocity of pipe flow is the critical point for generating turbulence. Then, it is shown how flattening the velocity profile leads to the elimination of the point of inflection on the velocity profile of pipe flows to delay turbulent transition. It is also clarified why this technique is not effective at higher Reynolds number because the flattened velocity profile violates the criterion for flow stability relating to transition to turbulence.

Article History

Received January 29, 2024
Revised April 21, 2024
Accepted May 22, 2024
Available online September 1, 2024

Keywords:

Pipe flow
Turbulent transition
Flattened velocity profile
Point of inflection
Energy gradient theory

1. INTRODUCTION

Two types of states of flow have been observed in nature as well as in engineering applications, i.e., laminar and turbulent flows (Schlichting & Gersten, 2017; Dou, 2022b). Unlike laminar flows, turbulent flows can produce a large drag force and consume more energy while transporting the fluid. Laminar flows are thus generally preferred in the design of airplanes, cars, and ships as well as in the transportation of various fluids through pipelines. One of the aims to study turbulence is to control the states of flow in military and industrial applications through various means. Developing a method to control the flow is thus important for reducing the drag force.

In this study, we use the energy gradient theory to demonstrate why the point of inflection on the profile of velocity of pipe flow is the critical point for generating turbulence. Further, we show that flattening the velocity profile leads to the elimination of the point of inflection, and thus enhances the stability of pipe flow to delay the transition to turbulence.

Hof et al. (2010a) experimentally and numerically examined whether a turbulent puff in a pipe can be removed or delayed by flattening the profile of the upstream velocity at a low Reynolds number. Their results showed that the point of inflection on the velocity profile is the essence of a turbulent spot or puff in pipe flow, and removing it causes the puff to collapse. Hof et al. (2010a) used a second puff to flatten the velocity profile upstream of the original puff (to be removed), and were able to successfully manipulate the flow. The point of inflection at the rear of the original puff (downstream of the second puff) was delayed as a result. This method for controlling the generation of turbulence offers promise for drag reduction in engineering and industrial applications.

Hof et al. (2010a) argued that the transport of the streamwise vorticity, which is given by the cross-sectional average of the product of the magnitude of the axial vorticity and the relative motion with respect to the mean velocity, $\langle|\omega_z|(u_z-U)\rangle$, dominates in terms of sustaining the point of inflection, and this in turn leads to the instability that leads to the regeneration of vorticity. Here, ω_z, u_z, and U in the above represents the axial vorticity, axial velocity, and the average axial velocity,

respectively. The results of their simulations showed that the strongest point of inflection coincides with the location of the vorticity production, at which the turbulent kinetic energy reaches its maximum after the point of inflection, thus indicating that turbulence had indeed been sustained by the instability of the point of inflection. This leads to the idea of delaying turbulence by removing the point of inflection.

Inflectional instability derived from inviscid flows (Rayleigh, 1880) has been used in past work to explain the transition/generation of turbulence in various flows (Kline et al., 1967; Robinson, 1991; Panton, 2001). However, this interpretation is based on the analysis of the Euler equation of an inviscid fluid, whereas the flow through a pipe is viscous flow that can be described only by using the Navier–Stokes equation.

Dou (2006, 2011, 2021, 2022a, b), Dou and Khoo (2009, 2010, 2011), and Dou et al. (2008) proposed the energy gradient theory to analyze flow stability and turbulent transition. For pressure-driven flow at a high Reynolds number, it is found that the inflection point on the velocity profile can be induced when a flow is subjected a disturbance. It is proved that the inflection point on the velocity profile is a singular point and it may results in flow instability and turbulent transition at sufficient large disturbance.

Dou (2021, 2022a, b) proved that the necessary and sufficient condition for turbulence generation/ turbulence transition is the appearance of singular point (velocity discontinuity) of the Navier-Stokes equation in flow field. The theory has obtained agreement with the available experimental results. For pressure-driven flows, this singularity corresponds to the position in the flow field where the Laplace operator is zero.

For a plane Poiseuille flow, the Laplace operator is given by

$$\nabla^2 u = \frac{\partial^2 u}{\partial x^2} + \frac{\partial^2 u}{\partial y^2} + \frac{\partial^2 u}{\partial z^2}.$$

If the flow is fully developed and uniform along the spanwise direction, $\partial^2 u / \partial x^2 = 0$ and $\partial^2 u / \partial z^2 = 0$. Thus, the point at which the Laplace operator is zero corresponds to the point of inflection on the velocity profile, $\partial^2 u / \partial y^2 = 0$. If the flow is not uniform along the spanwise direction, because the streamwise velocity is of the main flow, the last two terms of the Laplace operator have very small values, and the point where the Laplace operator is zero is located close to the point of inflection on the velocity profile.

The Laplace operator in case of the pipe Poiseuille flow is

$$\nabla^2 u = \frac{1}{r}\frac{\partial u}{\partial r} + \frac{\partial^2 u}{\partial r^2} + \frac{\partial^2 u}{r^2 \partial \theta^2} + \frac{\partial^2 u}{\partial z^2}.$$

If the flow is fully developed and axisymmetric, $\partial^2 u / \partial z^2 = 0$, $\partial^2 u / (r^2 \partial \theta^2) = 0$. Because $\partial u / (r \partial r)$ is very small near the point of inflection on the velocity profile, the point at which the Laplace operator is zero is located close to the point of inflection on the velocity profile, $\partial^2 u / \partial r^2 = 0$. If the flow is not axisymmetric, the last two terms of the Laplace operator are very small because the streamwise velocity is the main flow, and the point at which the Laplace operator is zero is close to the point of inflection on the velocity profile of the flow. Therefore, if there is a point of inflection on the velocity profile in case of circular pipe flow, singularity inevitably appears near the point of inflection.

According to the energy gradient theory (Dou, 2006, 2011, 2021, 2022a, b), when the velocity profile of the flow in a pipe is flattened, the maximum of the energy gradient function K decreases, which enhances the stability of flow. The appearance of the point of inflection is delayed, because of which the turbulent transition is extended to higher Reynolds number (Re). Therefore, the transition to turbulence can be controlled by manipulating the magnitude of the energy gradient function K.

In this study, we use the energy gradient theory to characterize the behavior of the flow field through a pipe. We quantitatively describe the mechanism to stabilize the flow by flattening its velocity profile. The flow is assumed to be axisymmetric laminar flow that is solved analytically by using the Navier–Stokes equation with a varying control parameter to flatten the velocity profile. The results show that flattening the velocity profile of the flow reduces the maximum of the energy gradient function and therefore stabilizes the flow. The occurrence of the point of inflection on the velocity profile is delayed, and the critical Reynolds number for turbulent transition increases. Following this, we clarify the physical mechanism of the failure of the technique used to control turbulence at higher values of Re (Re>~3000). The motivation of our research here is to offer a plausible account of this phenomenon. Finally, our work here based on the energy gradient theory supports the idea in Hof et al. (2010a) that removing the point of inflection on the velocity profile can delay the transition to turbulence in pipe flows within a certain range of the Reynolds number.

2. ENERGY GRADIENT THEORY APPLIED TO PIPE FLOW

Dou and co-authors (Dou, 2006; Dou et al., 2008; Dou, 2011, 2021) proposed an energy gradient theory to clarify the mechanism of transition of wall-bounded flows from laminar flow to turbulence. According to this approach, the interaction between the disturbance and the base flow leads to variations in the total mechanical energy of the disturbed particles of fluid and the evolution of the average velocity profile. The relative magnitude of the total mechanical energy gained by the particles and the loss of energy owing to viscous friction in each cycle of disturbance dominates the amplification or decay of the disturbance. For a given base flow, the criterion of stability is as follows (Dou, 2011),

$$K\frac{v'_m}{u} < Const \qquad (1)$$

and

$$K = \frac{\partial E / \partial n}{\partial H / \partial s} \tag{2}$$

where K is a dimensionless field variable (function) that is expressed as the ratio of the transversal gradient of the total mechanical energy to the rate of energy loss along the streamline, and can be calculated from the Navier–Stokes equation. In Eq. (2), $E = p + \frac{1}{2}\rho V^2$ is the total mechanical energy per unit volume of fluid when the gravitational force is neglected, s is along the streamwise direction, while n is along the direction normal to the streamline. H is the loss of the total mechanical energy per unit volume of fluid along the streamline over a finite length, ρ is the density of the fluid, u is the streamwise velocity of the main flow, and v'_m is the amplitude of disturbance in the velocity along the direction normal to the wall.

The energy gradient function K is a variable of space and time, and is actually a **local Reynolds number** (Dou, 2006, 2021, 2022a, b). Its magnitude is important but its sign does not matter.

For pressure-driven flows, the rate of the energy loss (total mechanical energy) along the streamline is equal to the reduction in the total mechanical energy along the streamline. Then, Eq. (2) can be rewritten as (Dou, 2006),

$$K = \frac{\partial E / \partial n}{\partial E / \partial s}. \tag{3}$$

where $\partial E / \partial s$ is the reduction in the total mechanical energy along the streamline over a finite length.

The magnitude of K is proportional to the global Reynolds number ($\mathrm{Re} = \rho U(2R)/\mu$) for a given geometry for all types of flows (Dou, 2006, 2011). Thus, the criterion given in Eq. (1) can be rewritten as (Dou, 2011):

$$\mathrm{Re}\frac{v'_m}{u} < Const. \tag{4}$$

For a given geometry of flow, U is the characteristic velocity (mean velocity here) that is generally a function of u. Thus, Eq. (4) can be rewritten as (Dou, 2011):

$$\mathrm{Re}\frac{v'_m}{U} < Const \text{ or } \left(\frac{v'_m}{U}\right)_c \sim (\mathrm{Re})^{-1}. \tag{5}$$

This scaling is in excellent agreement with the results of experiments on pipe flow with a normally injected disturbance (Hof et al., 2003; Peixinho & Mullin, 2007). The basic flow is assumed to be maintained as parallel flow during modeling once the perturbation has been input, and is unaffected by the disturbance (Dou, 2011). Therefore, Eq. (4) or Eq. (5) is applicable only to injection-induced disturbance, and is not suitable for the push–pull disturbance, considered by Peixinho and Mullin (2007), or other types of disturbances (Lundbladh et al., 1994; Chapman, 2002). In case of push–pull disturbance, the basic flow is locally non-parallel. More importantly, the push–pull disturbance is not a free perturbation, but involves the input of external work. In this case, the boundary condition of the system changes.

The energy gradient function K is a variable of the flow field. For a given flow field, there is a maximum of K at which the flow is the most unstable. Thus, the maximum of K and the point at which it occurs can be considered to be indications of the most dangerous position for the generation of turbulence.

According to the criterion of stability given in Eq. (1), $K\left(v'_m / u\right) < Const$, non-linear interactions between the disturbance and the base flow (where both K and $\left(v'_m / u\right)$ vary with time) lead the flow to the critical condition of turbulent transition. The streamwise velocity oscillates intensely at the most dangerous position for the generation of turbulence in the critical condition, and the mean flow exhibits a point of inflection under the ensuing disturbance. The contribution of the base flow to this instability is the magnitude of the function K. Equation (1) shows that the flow is expected to be more unstable at locations where the magnitude of K is larger under the same level of normalized perturbation $\left(v'_m / u\right)$. The amplitude and the position of the initial oscillation should be associated with the maximum of K in the flow domain, (K_{max}), for a given uniform disturbance. If the disturbance is not uniform, this position may slightly deviate from the location of K_{max}.

Equation (1) expresses the critical condition for the transition to turbulence under variations of the energy gradient function and the dimensionless amplitude of the disturbance. Under the critical condition, the maximum of K is inversely proportional to the dimensionless amplitude of disturbance.

Figure 1 shows the average velocity profiles of laminar flow, transitional flow, and turbulent flow through a pipe. The velocity distribution of a laminar flow through a pipe can be expressed as (Dou, 2006, 2011):

$$u = u_0\left(1 - \frac{r^2}{R^2}\right) \tag{6}$$

The energy gradient function K of pipe flow can be obtained through the Navier–Stokes equation and Eq. (3):

$$K = \rho u \frac{\partial u}{\partial r} / \mu\left(\frac{1}{r}\frac{\partial u}{\partial r} + \frac{\partial^2 u}{\partial r^2}\right). \tag{7}$$

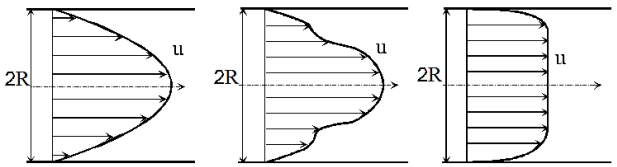

(a) (b) (c)

Fig. 1 Velocity profiles during the transition from laminar flow to turbulence in case of Poiseuille pipe flow, as observed in experiments and simulations. (a) Laminar flow. (b) Transitional flow. (c) Turbulence

Equation (7) is for laminar flow or transitional flow through a pipe since the denominator in Eq. (7) represents the drop of the total mechanical energy along a streamline. As the flow is subjected to disturbance, it becomes unsteady, and may even be non-axisymmetric. At some point, for example, at the point of inflection, the gradient of the total mechanical energy, $\partial E/\partial s$, along the streamline may become zero, and this point is a singular point (Dou, 2021). The value of the energy gradient function K is infinite at this point, and the capability of amplification in the disturbance is very large. This is the location at which a turbulent "burst" occurs, which leads to a peak pressure distribution at the said location.

Dou et al. (Dou, 2006, 2011, 2022b) have shown that the critical value of *K* for plane Poiseuille flow and pipe Poiseuille flow, determined from experimental data, is about 385. If *K* is lower than this value, turbulence cannot be generated regardless of the level of disturbance. The most unstable position for plane Poiseuille flow and pipe Poiseuille flow occurs at $y/h = \pm 0.58$ and $r/R = 0.58$, respectively, and this has been confirmed through experiments. Nishioka et al. (1975) used ribbon-induced disturbances in plane Poiseuille flow and showed that the average velocity profile exhibited intense oscillations (inflections) in the range of y/h= ± 0.50~0.62. Nishi et al. (2008) used normal injection as disturbance in pipe Poiseuille flow, and showed that the average velocity profile was subjected to intense oscillations (inflections) in the range of r/R=0.53~0.73 during the occurrence of transition in flow. These experimentally obtained locations have been shown to agree with those predicted by the energy gradient theory (0.58).

The energy gradient theory has also been shown to be valid for plane Couette flow (Dou & Khoo, 2011), Taylor–Couette flow (Dou et al., 2008), and boundary layer flow (Dou & Khoo, 2009), and has exhibited excellent agreement with the relevant experimental data provided in the literature.

The formation of streamwise vortices can be explained as follows: A disturbance with a finite amplitude causes the velocity profile to oscillate locally according to Eq. (1). The extent of this oscillation varies along the radial direction, and is the largest at about $r/R = 0.58$. The amplification in the disturbance at this location then causes the velocity profile to assume an inflectional feature. The velocity profile becomes unstable if Re is sufficiently large, while the pressure at this location decreases owing to the large magnitude of the disturbance-induced velocity because the mean pressure is constant along the radius. This low pressure, at about $r/R = 0.58$, induces a secondary flow on the cross-section that forms streamwise vortices. If the initial disturbance is uniform along the radial direction, the secondary flow is centered at $r/R = 0.58$. If the initial disturbance is non-uniform along the radial direction, the location of the secondary flow may deviate from $r/R = 0.58$. The secondary vortices on the cross-section have been clearly identified in experiments and simulations (Hof et al., 2010a), and sustain the presence of the point of inflection. The low pressure at the center of these vortices helps maintain the secondary vortices at a constant strength.

Dou (2021) discovered that there exists a singularity in the Navier–Stokes equation in case of the transition of channel flow, which explains the mechanism of transition from smooth laminar flow to turbulence. In case of channel flow, the singular point is located at the point of inflection on the velocity profile, while it is located *near* the point of inflection in case of pipe flow. The velocity becomes discontinuous at the singular point and a negative spike is formed, while the peak pressure occurs due to the conservation of the total mechanical energy. However, the discontinuity in velocity and the peak in pressure occur instantaneously during the disturbance.

Dou (2022a) analyzed the Poisson's equation to further confirm the above conclusions. The Navier–Stokes equation was written as a form of Poisson's equation to this end. The results showed that the position at which the Laplace operator is zero is the singular point of the Poisson equation, and corresponds to the location at which the viscous term vanishes, close to the point of inflection, in case of pipe flow.

We have mentioned above that Hof et al. (2010a) argued that the transport of the streamwise vorticity, given by the cross-sectional average of the product of the magnitude of the axial vorticity and the relative motion with respect to the mean velocity, $\langle|\omega_z|(u_z - U)\rangle$, governs the maintenance of the point of inflection, and in turn causes the instability that regenerates vorticity. In fact, the magnitude of $\langle|\omega_z|(u_z - U)\rangle$ needs to reach its maximum at the singular point predicted by the energy gradient theory, at which the fluctuation in velocity is the largest. Therefore, the energy gradient theory shares the idea which is similar to that proposed by Hof et al. (2010a).

3. CONTROLLING TRANSITION BY MANIPULATING K_{MAX}

Past work suggests that the transition to turbulence can be controlled by manipulating the function K (Dou, 2006; Dou & Khoo, 2010; Dou, 2022b). Flattening the velocity profile is one means to this end. We show below that a flattened velocity profile reduces the value of K_{max} in the domain and hence makes the flow more stable. Under the same conditions of disturbance, the transition to turbulence can then be extended or delayed to larger value of Re.

The steady Navier–Stokes equation for laminar pipe flow can be reduced as follows:

$$0 = -\nabla p + \mu \nabla^2 u + F \tag{8}$$

where ∇p is the pressure gradient and F is the body force. As is well known, the solution to the above equation is a parabola when the body force is neglected (Hagen–Poiseuille flow).

We can rewrite Eq. (8) as,

$$(\nabla p - F) = \mu \nabla^2 u \,. \tag{9}$$

If F is uniform along the radius, $(\nabla p - F) = Const$, where adding a body force is equivalent to reducing the pressure gradient, the velocity profile maintains a parabolic shape (case 1).

If F is non-uniform but smooth along the radius, and its maximum occurs at the centerline, this minimizes the value of $(\nabla p - F)$ at the centerline. In this case, F causes the velocity profile to flatten (case 2).

If F is non-uniform but smooth along the radius, and its minimum value occurs at the centerline, this maximizes the value of $(\nabla p - F)$ at the centerline. In this case, F causes the velocity profile to become stretched (case 3).

In case of the flattening of the velocity profile (case (2)), the solution to the Navier–Stokes equation for pipe flow under a pressure gradient and a certain volumetric force can be expressed by a series of even power functions of the ratio of the radius:

$$u = u_0 \left[\left(1 - \frac{r^2}{R^2}\right) + \varepsilon \left(1 - \frac{r^4}{R^4}\right) + \varepsilon_1 \left(1 - \frac{r^6}{R^6}\right) + \varepsilon_2 \left(1 - \frac{r^8}{R^8}\right) + \ldots \right] \tag{10}$$

where ε, ε_1, ε_2 …, are constant parameters. In case of a small amount of flattening of the velocity profile, only the leading terms are sufficient, but higher-order terms are required for a large amount of flattening of the velocity profile.

When the body force is not large, the flattening of the velocity profile is limited to within a certain range of F. Under such conditions, Eq. (10) can be rewritten as follows for convenience:

$$u = u_0 \left(1 - \frac{r^2}{R^2}\right) + \varepsilon u_0 \left(1 - \frac{r^4}{R^4}\right) \tag{11}$$

where $\varepsilon = 0$ corresponds to a parabolic profile. The velocity distributions under various values of ε are shown in Fig. 2. The average velocity profile is determined here under a constant rate of flow and various values of ε. It is clear that the velocity profile is gradually flattened with increasing values of ε.

Hof et al. (2010b) simulated the laminar flow with a flattened velocity profile and input a volumetric force to the system by using the full Navier–Stokes equation. They used a parameter expressing the reduction in velocity at the centerline, $\alpha = 0.15$, for the flattening of the velocity profile. This means that the maximum velocity at the centerline had decreased by 15%. According to Eq. (11), if the maximum velocity is reduced by 15%, $\varepsilon = 1.1538$ such that the average velocity (or flow rate) remains unchanged. This value can be obtained as follows.

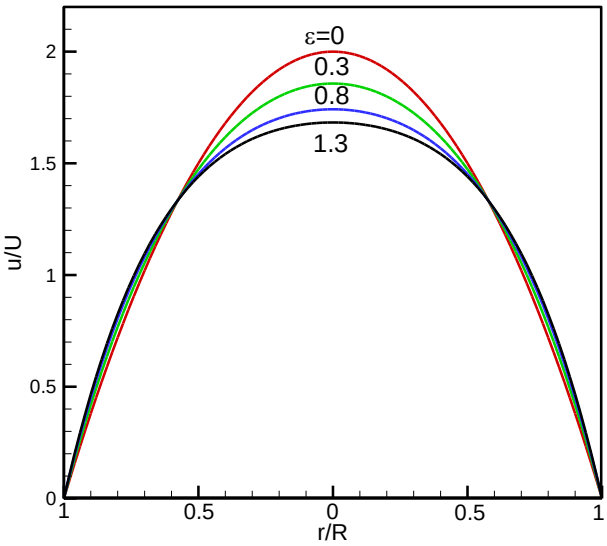

Fig. 2 Velocity profiles for various values of ε and a constant average velocity U. Here $\varepsilon = 0$ corresponds to a parabolic profile ($u_0 / U = 2$)

The average velocity of the flattened velocity profile in Eq. (11) is $U = u_0(\frac{1}{2} + \frac{2}{3}\varepsilon)$, while the velocity at the centerline is $u_0 + \varepsilon u_0$. The average velocity of pipe Poiseuille (parabolic) flow is $U = \frac{1}{2}u_0$, while the velocity at the centerline is u_0 in this case. Thus, for the maximum velocity at the centerline to decrease by 15%, we have

$$u_0 + \varepsilon u_0 = (1 - 0.15) u_{0P} \,. \tag{12}$$

For the average velocity to remain unchanged after the velocity profile has been flattened, we have,

$$u_0(\frac{1}{2} + \frac{2}{3}\varepsilon) = \frac{1}{2}u_{oP}, \tag{13}$$

where u_{oP} denotes the velocity of the Poiseuille (parabolic) profile at the centerline in case of pipe flow. We obtain $\varepsilon = 1.1538$ from the solution of Eqs. (12) and (13).

A comparison between the results of Eq. (11) for a 15% reduction in the maximum velocity and those of the simulation by Hof et al.(2010a) is shown in Fig. 3. It is clear from it that the two profiles are nearly identical. Thus, the velocity profile represented by Eq. (11) can be considered to be a solution to the Navier–Stokes equation for $\varepsilon = 1.1538$.

By introducing Eq. (11) into Eq. (3), we obtain,

$$K = \frac{1}{4}\mathrm{Re}\frac{\frac{r}{R}\left(1 + 2\varepsilon\frac{r^2}{R^2}\right)\left[1 - \frac{r^2}{R^2} + \varepsilon\left(1 - \frac{r^4}{R^4}\right)\right]}{\left(1 + 4\varepsilon\frac{r^2}{R^2}\right)\left(\frac{1}{2} + \frac{2}{3}\varepsilon\right)}, \tag{14}$$

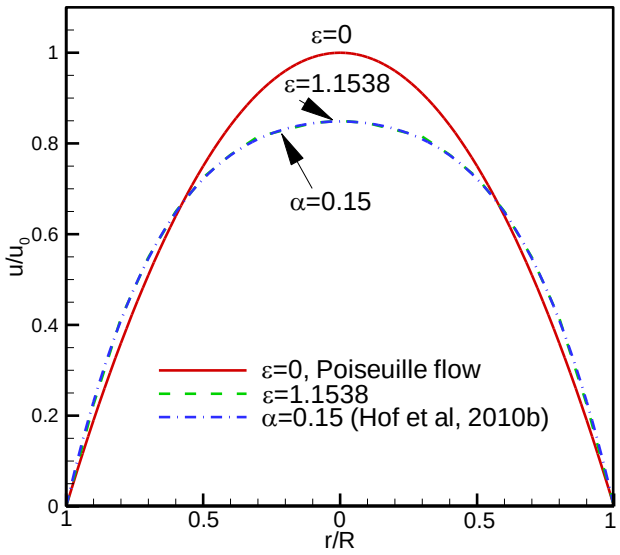

Fig. 3 Comparison of velocity profiles obtained from Eq. (8) with those in the numerical simulations by Hof et al. (2010b). For all cases, the average velocity U was kept unchanged. The case of $\varepsilon = 0$ corresponds to the parabolic profile of velocity ($u_0 / U = 2$). The dotted–dashed line is taken from Hof et al. (2010b) for $\alpha = 0.15$, i.e., the maximum velocity decreased by 15%. For the same reduction in the maximum velocity, $\varepsilon = 1.1538$ from Eq. (8)

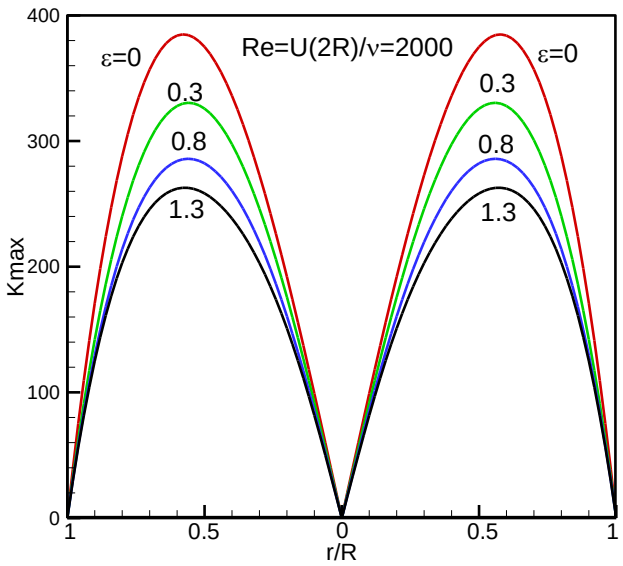

Fig. 4 Distribution of K along the radial direction for various values of ε (based on Eq. (8))

where the Reynolds number is $\mathrm{Re} = \rho U(2R)/\mu$.

The velocity distribution in pipe flow can be modified by adjusting the parameter ε. With increasing values of ε, the velocity distribution is gradually flattened. Thus, the maximum of the energy gradient function K is reduced according to Eq. (14), and the stability of pipe flow can be enhanced by adjusting ε.

Equation (14) gives a general formulation to predict flow stability, and is an exact formulation to predict the onset of the process of transition from laminar flow to turbulence. When the value of the denominator of K in Eq. (14) is close to zero during the development of transient flow (meaning singularity occurrence), this represents the beginning of the generation of turbulence.

4. RESULTS OF CALCULATIONS WITH VARYINGLY FLATTENED VELOCITY PROFILES

Figure 4 shows the distribution of the function K along the radius of the pipe at various values of ε for Re=2000. It is evident that the value of K_{max} decreases with increasing value of ε. The location of K_{max} occurrs at around r/R=0.56~0.60, and does not vary much with ε. These observations suggest that an increase in ε enhances the stability of laminar flow, and the location of the most unstable position remained almost unchanged at about $r/R = 0.58$. This is why the flow is stabilized and turbulent transition is delayed when the flow has been flattened (ε increased).

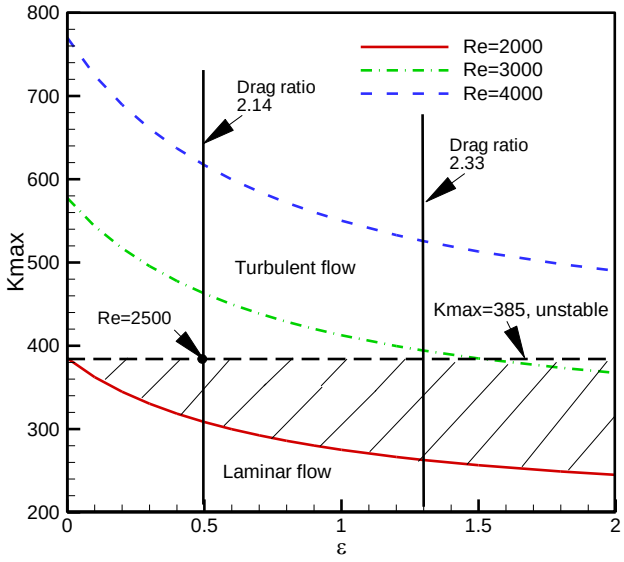

Fig. 5 Maximum of K versus ε for pipe flow. According to the energy gradient theory, turbulence can occur only at $K_{max} \geq 385$ for parallel flows (Dou, 2006, 2011). If K_{max} is reduced, the transition to turbulence is delayed. The drag ratio is defined as $\bar{D} / \bar{D}_{\varepsilon=0}$, where $\bar{D}$ expresses the drag for the flattened velocity profile of laminar flow, and $\bar{D}_{\varepsilon=0}$ denotes the original laminar parabolic profile. The shaded area is the zone that can be modified to laminar flow by flattening the velocity profile, which depends on the magnitudes of Re and ε

Figure 5 shows the maximum of K versus the value of ε at different Reynolds numbers. K_{max} increases with increasing value of Re. For Re=4000, the value of K_{max} is always larger than 500, up to a large value of ε=2, and it tends toward a value of 408 as ε approaches infinity. For Re=3000 and ε=1.0, K_{max} is 413, which is larger

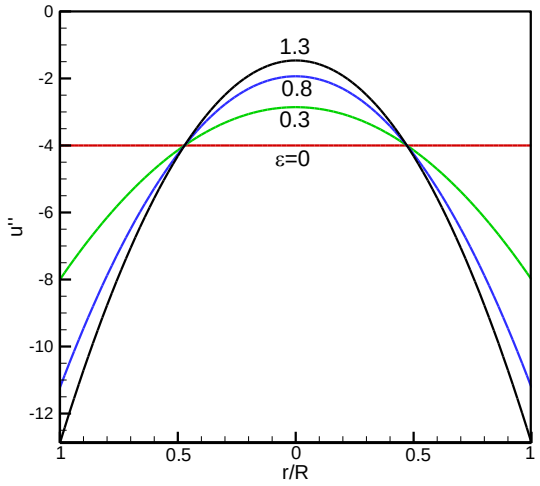

Fig. 6 Second derivatives of the streamwise velocity versus the radial direction at various values of ε while keeping the average velocity U unchanged (u'' is normalized by U/R^2)

than the critical value of K_c=385 for turbulent transition in the original pipe flow, and leads to turbulence. At this Reynolds number, even using ε =2.0 yields a value of K_{max} of 368, which is near the critical value of 385. Thus, it becomes difficult to delay the turbulent transition by flattening the velocity profile at Re=3000, even with a large value of ε =2. Hof et al. (2010a, b) found that flattening the velocity profile to delay turbulence works well for sufficiently small values of Re ($\mathrm{Re} \approx 2000$), but fails when Re is larger ($\mathrm{Re} \geq 2500$). The variation in K_{max} with Re as shown depicted in Fig. 5 aptly explains these phenomena, which are further discussed below.

Figure 6 shows the distributions of the second derivative of the velocity u with respect to the radius (i.e., u'') for various values of ε . It is seen that u'' becomes more non-uniform as the velocity is increasingly flattened: $|u''|$ decreases at the centerline but increases near the wall. For ε =0.3, the value of $|u''|$ at the wall doubles. This means that the drag of the laminar flow has significantly increased. At larger values of ε , the value of $|u''|$ at the wall increases further. This means that the drag of the laminar flow significantly increases at large values of ε in Eq. (11).

The dimensionless drag on the wall of the pipe can be calculated by the following equation:

$$\bar{D} = \frac{\mu\left(\frac{1}{r}\frac{du}{dr} + \frac{d^2u}{dr^2}\right)}{\mu\frac{U}{R^2}}. \tag{15}$$

By using Eq. (11), Eq. (15) can be rewritten as,

$$\bar{D} = \frac{4\left(1+4\varepsilon\frac{r^2}{R^2}\right)}{\left(\frac{1}{2}+\frac{2}{3}\varepsilon\right)}. \tag{16}$$

Table 1 Variations in the dimensionless drag force on the flattened velocity profile of laminar flow versus values of ε

ε	K_{max} (Re=3000)	$\bar{D}$	$\bar{D}/\bar{D}_{\varepsilon=0}$
0	577	8	1
0.3	495	12	1.5
0.8	429	16.2	2.1
1.3	394	18.1	2.3
1.5	385	18.7	2.35
2.0	367	19.6	2.45
2.5	356	20.3	2.54
3.0	347	20.8	2.60

On the wall, r=R, we then have,

$$\bar{D} = \frac{4(1+4\varepsilon)}{\left(\frac{1}{2}+\frac{2}{3}\varepsilon\right)}. \tag{17}$$

Table 1 provides a comparison between the drag force of the modified (flattened) velocity profile of laminar flow with that of its original (parabolic) velocity profile. For Re=3000, the flow transitioned to turbulence (because K_{max}>385), even when we used a large value of ε (say at 1.5) to flatten its velocity profile. At ε =1.5, the drag increased to 2.33 times that of the parabolic laminar flow. For values of Re larger than 3,000, the scenario is worsened, and there is little likelihood of delaying turbulence and reducing the drag by using the technique proposed by Hof et al. (2010a, b). Therefore, this technique (Hof et al., 2010a) is valid only at small Reynolds numbers (i.e., about 2,000 or slightly larger), and is not applicable to large values of Re (Re>~3000). Strictly speaking, Hof et al. found that this technique is valid only for Re<2500 (Hof et al., 2010a, b).

Equation (15) shows that the drag ratio $\bar{D}/\bar{D}_{\varepsilon=0}$ is dependent only on ε , and is unrelated to Re. $\bar{D}$ is the drag of the modified (flattened) velocity profile of laminar flow while $\bar{D}_{\varepsilon=0}$ is that of the original (parabolic) velocity profile of laminar flow in a pipe. Fig. 5 shows that if $\bar{D}/\bar{D}_{\varepsilon=0}$ is increased for the flattened velocity profile in pipe flow to 2.14, the required value of ε is 0.5. To obtain K_{max}=385 and ensure laminar flow, the maximum allowable Re is 2,500. At value of Re larger than 2,500, a larger value of ε needs to be applied. As shown in Table 1, however, a larger ε leads to a larger drag associated with laminar flow. The shaded area in Fig. 5 represents the zone that can be modified to laminar flow by flattening the velocity profile via the energy gradient theory (Dou, 2011), where this depends on the magnitudes of Re and ε .

Table 2 shows the values of ε required to delay the transition to turbulence and the locations of K_{max} at various values of Re. It is clear that the value of ε required to delay the transition to turbulence increased with Re. For Re=2800, the required value of ε was larger than one, while it was larger than 1.5 for Re=3000. For even larger values of Re ($\mathrm{Re} \geq 4000$), the required

Table 2 Values of ε required to delay the transition to turbulence, and the locations of the K_{max} at various values of Re

Re	ε	$(r/R)_{K\max}$
2000	0	0.58
2200	0.162	0.56
2500	0.49	0.56
2800	0.985	0.56
3000	1.5	0.58
3500	4.95	0.62
3700	13.0	0.64
4000	N/A	0.66

values of ε became impossibly large such that reducing the value of K_{max} to below 385 became impossible (it tended asymptotically to 401 with infinite values of ε at Re=4000). This means that it is very difficult to delay the transition to turbulence at larger values of Re by flattening the velocity profile of flow. Table 2 also shows that K_{max} was located at around r/R=0.56~0.66 for Re=2000~4000. At larger values of Re, its location moved slightly toward the wall of the pipe.

Experiments on pipe flows (Fargie & Martin, 1971) have shown that the shape of the velocity profile is closely related to the magnitude of the drag force. Therefore, the variation in drag should be carefully considered when using the flattening technique.

In addition, the flow in a pipe system may be subject to transient behavior due to variations in the pressure. The shape of the velocity profile in such systems changes over time, because of which the shear stress on the wall varies as well (Brunone & Berni, 2010), and this in turn leads to temporally variable drag. We considered the average profile of flow in this analytical examination.

Experimental study of the transient flow in a coiled pipe using PIV has shown that the energy dissipation is different for steady-state and unsteady-state flows (Brito et al., 2016). In particular, the flow may undergo local accelerations or decelerations in transient flow as well as occurrence of asymmetric flow. This means that the key features of the unsteady-state flow should be carefully considered in estimation of the pressure drop in pipe flows.

5. CONCLUSIONS

In this study, we examined the inflectional instability of pipe flow and the stabilizing effect of a flattened velocity profile on it. The flattened velocity profile helped eliminate the point of inflection on the velocity profile of flow in a certain range of value of the Reynolds number. The energy gradient theory can explain and predict the mechanism of this stabilizing effect as evidenced in experiments by Hof et al. (2010a). The conclusions of this study can be summarized as follows:

(1) We used the energy gradient theory to reasonably explain the stabilizing mechanism of the flattened velocity profile, and showed why this is effective only at low values of Re. The mechanism of initial streamwise vortices was also discussed. We found that flattening the velocity profile reduced the maximum of the energy gradient function K and stabilized the flow. The occurrence of the point of inflection on the velocity profile was delayed, and the critical Reynolds number for the transition to turbulence moved to a larger value.

(2) Although the proposed technique is useful for stabilizing the flow and delaying the transition to turbulence, it has three disadvantages (Hof et al., 2010a, b): (a) Energy is required to broaden the velocity profile of the base flow, such as that of liquid metals or plasmas via magnetic fields, as has been suggested by Hof et al. (2010a). (b) The flattened velocity profile increases the drag force associated with laminar flow owing to a steeper gradient near the wall. (c) The proposed control over turbulence is effective only at low Reynolds numbers (close to 2000). At large values of Re, not only can the turbulence not be delayed, but the drag force associated with laminar flow also significantly increases. For example, at Re=3000 and ε =1.3, K_{max} was about 394, which is already larger than the critical value of K_c=385 for the original laminar parabolic flow, such that the system still tended toward turbulence. Meanwhile, the drag increased to 2.3 times that of parabolic laminar profile, as shown in Table 1.

(3) We used the energy gradient theory to support the idea proposed by Hof et al. (2010a), that removing the point of inflection on the velocity profile of pipe flows can delay the transition to turbulence. This is because a singular point always exists near the point of inflection. Eliminating the point of inflection is to remove a singular point, which stabilizes the flow while avoiding occurrence of a turbulent "burst."

(4) The instability induced by the point of inflection on the velocity profile was analyzed based on the Navier–Stokes equation by using the energy gradient theory. This is not related to the instability of inviscid flow, which is described by the Euler equation (Rayleigh, 1880).

Finally, it should be pointed out that only flows in circular pipe with smooth surface are considered when the analytical method is applied in the present work. Effect of the wall roughness on the flow behavior would be considered in future studies.

ACKNOWLEDGEMENTS

The authors thank Prof. B. C. Khoo from National University of Singapore and Prof. Z.-S. She from Peking University for their helpful comments.

CONFLICT OF INTEREST

The authors declare that there is no any financial or non-financial interest in this paper.

AUTHORS CONTRIBUTION

C. Q. Zhou formulated part of the equations, completed part of the calculations, and revised the

manuscript. **H. L. Zhao** joined the discussions on applications of the technique delaying turbulent transition and participated in the revision of the manuscript. **H.-S. Dou** proposed the idea, administrated the project, formulated part of the equations, did part of calculations, and wrote the first manuscript of this paper.

REFERENCES

Brito, M., Sanches, P., Ferreira, R. M. L., & Covas, D. I. C. (2016). Experimental study of the transient flow in a coiled pipe using PIV. *ASCE Journal of Hydraulic Engineering*, *143*, 04016087. https://doi.org/10.1061/(ASCE)HY.1943-7900.0001253

Brunone, B., & Berni, A. (2010). Wall shear stress in transient turbulent pipe flow by local velocity measurement. *ASCE Journal of Hydraulic Engineering*, *136*, 716-726. https://doi.org/10.1061/(ASCE)HY.1943-7900.0000234

Chapman, S. J. (2002). Subcritical transition in channel flows. *Journal of Fluid Mechanics*, *451*, 35-97. https://doi.org/10.1017/S0022112001006255

Dou, H. S. (2006). Mechanism of flow instability and transition to turbulence. *International Journal of Non-Linear Mechanics*, *41*(4), 512-517. https://doi.org/10.1016/j.ijnonlinmec.2005.12.002

Dou, H. S. (2011). Physics of flow instability and turbulent transition in shear flows. *International Journal of Physical Science*, *6*(6), 1411-1425. http://arxiv.org/abs/physics/0607004.

Dou, H. S. (2021). Singularity of Navier-Stokes equations leading to turbulence. *Advances in Applied Mathematics and Mechanics*, *13*(3), 527-553. https://doi.org/10.4208/aamm.OA-2020-0063

Dou, H. S. (2022a). No existence and smoothness of solution of the Navier-Stokes equation. *Entropy*, *24*(2), 339. https://doi.org/10.3390/e24030339

Dou, H. S. (2022b). *Origin of turbulence-energy gradient theory*. Springer. https://link.springer.com/book/10.1007/978-981-19-0087-7

Dou, H. S., & Khoo, B. C. (2009). Mechanism of wall turbulence in boundary layer flows. *Modern Physics Letters B*, *23* (3), 457-460. http://arxiv.org/abs/0811.1407

Dou, H. S., & Khoo, B. C. (2010). Criteria of turbulent transition in parallel flows. *Modern Physics Letters B*, *24* (13),1437-1440. http://arxiv.org/abs/0906.0417

Dou, H. S., & Khoo, B. C. (2011). Investigation of turbulent transition in plane Couette flows using energy gradient method. *Advances in Applied Mathematics and Mechanics*, *3*(2), 165-180. http://arxiv.org/abs/nlin.CD/0501048

Dou, H. S., Khoo, B. C., & Yeo K. S. (2008). Instability of Taylor-Couette flow between concentric rotating cylinders. *International Journal of Thermal Sciences*, *47*(11), 1422-1435. https://doi.org/10.48550/arXiv.physics/0502069

Fargie, D., & Martin, B. W. (1971). Developing laminar flow in a pipe of circular cross-section. *Proceedings of the Royal Society London A*, *321*, 461-476. https://www.jstor.org/stable/77808

Hof, B., de Lozar, A., Avila, M., Tu, X., & Schneider, T.M. (2010a). Eliminating turbulence in spatially intermittent flows. *Science*, *327*(5972), 1491-1494. https://www.science.org/doi/10.1126/science.1186091

Hof, B., de Lozar, A., Avila, M., Tu, X., & Schneider, T.M. (2010b). Eliminating turbulence in spatially intermittent flows: supporting online materials. *Science*, *327*(5972), 1491-1494. www.sciencemag.org/cgi/content/full/327/5972/1491/DC1 /Hof-SOM.pdf

Hof, B., Juel, A., & Mullin, T. (2003). Scaling of the turbulence transition threshold in a pipe. *Physical Review Letters*, *91*, 244502. https://doi.org/10.1103/PhysRevLett.91.244502

Kline, S. J., Reynolds, W. C., Schraub, F. A., & Runstadler, P.W. (1967). The structure of turbulent boundary layers. *Journal of Fluid Mechanics*, *30*, 741-773. http://journals.cambridge.org/abstract_S0022112067001740

Lundbladh, A., Henningson, D. S., & Reddy, S. C. (1994). Threshold amplitudes for transition in channel flows. *Transition, turbulence and Combustion*, *1*, 309-318. http://doi.org/10.1007/978-94-011-1032-7_30

Nishi, M., Unsal, B., Durst, F., & Biswas, G. (2008). Laminar-to-turbulent transition of pipe flows through puffs and slugs. *Journal of Fluid Mechanics*, *614*, 425-446. http://doi.org/10.1017/S0022112008003315

Nishioka, M., Iida, S., & Ichikawa, Y. (1975). An experimental investigation of the stability of plane Poiseuille flow. *Journal of Fluid Mechanics*, *72*(4), 731-751. https://doi.org/10.1017/S0022112075003254

Panton, R. L. (2001). Overview of the self-sustaining mechanisms of wall turbulence. *Progress in Aerospace Sciences*, *37*, (4), 341-383. https://arc.aiaa.org/doi/10.2514/6.2001-2911

Peixinho, J., & Mullin, T. (2007). Finite-amplitude thresholds for transition in pipe flow. *Journal of Fluid Mechanics*, *582*, 169-178. https://doi.org/10.1017/S0022112007006398

Rayleigh, L. (1880). On the stability or instability of certain fluid motions. *Proceedings of the London*

Mathematical Society, s1-11, 57–72. https://doi.org/10.1112/plms/s1-11.1.57

Robinson, S. K. (1991). Coherent motion in the turbulent boundary layer. *Annual Review of Fluid Mechanics*, *23*, 601-639. https://www.annualreviews.org/doi/10.1146/annurev.fl.23.010191.003125

Schlichting, H., & Gersten, K. (2017). *Boundary-layer theory*. Springer. https://link.springer.com/book/10.1007/978-3-662-52919-5